

## Influence of tire rubber waste on the fire behavior of gypsum coatings of construction and structural elements

F.J. Castellón<sup>a</sup>✉, M. Ayala<sup>a</sup>, M. Lanzón<sup>b</sup>

a. Department of Structures, Construction and Graphic Expression, Technical University of Cartagena, (Murcia, Spain)  
b. Department of Architecture and Building Technology, Technical University of Cartagena, (Murcia, Spain)

✉: franciscojose.castellon@upct.es

Received 21 April 2021  
Accepted 1 September 2021  
Available on line 15 March 2022

**ABSTRACT:** The addition of inorganic expanded aggregates, such as perlite or vermiculite is well known in gypsum plasters. However, the reuse of organic wastes in coatings like plasters and renders has been poorly studied. This paper shows the effect of tire rubber wastes on the mechanical properties and fire performance of gypsum plasters. The rubber waste was added to the mixture in mass percentages of 14.50% (C1) and 46.60% (C2). Flexural and compressive strength of plasters made with rubber wastes was visibly reduced as well as their surface hardness (Shore C). In addition, fire tests produced major damages through the entire 2 cm thickness of samples containing rubber wastes, as it was corroborated by X ray diffraction (XRD) and Thermogravimetric (TG) analysis. The heat transfer due to fire exposure modified considerably the chemical composition of plasters, since, on the non-exposed face to fire, the amount of gypsum ( $\text{CaSO}_4 \cdot 2\text{H}_2\text{O}$ ) equivalent to mass loss obtained by TG due to water released by these plasters made with rubber wastes, was 5.4-7.2 lower than that of conventional plasters. The results suggest that certain wastes may reduce the efficiency of gypsum plasters in protecting underneath construction and structural elements against fire.

**KEYWORDS:** Gypsum; Tire rubber waste; Fire; Temperature; Passive protection.

**Citation/Citar como:** Castellón, F.J.; Ayala, M.; Lanzón, M. (2022) Influence of tire rubber waste on the fire behavior of gypsum coatings of construction and structural elements. *Mater. Construcc.* 72 [345], e275. <https://doi.org/10.3989/mc.2022.06421>.

**RESUMEN:** *Influencia de los residuos de caucho de neumáticos en el comportamiento al fuego de revestimientos de yeso de elementos constructivos y estructurales.* La adición de agregados inorgánicos expandidos, como la perlita o la vermiculita, se conoce bien en los enlucidos de yeso. Sin embargo, la reutilización de residuos orgánicos en este tipo de revestimientos ha sido poco estudiada. Este trabajo muestra el efecto de los residuos de caucho de neumáticos fuera de uso sobre las propiedades mecánicas y el comportamiento frente al fuego de los revestimientos de yeso. El residuo de caucho se añadió a la mezcla en porcentajes en masa del 14.50% (C1) y 46.60% (C2). La resistencia a flexión y a compresión de los yesos adicionados con residuos de caucho se redujo visiblemente, así como su dureza superficial (Shore C). Además, los ensayos de fuego produjeron daños importantes en todo el espesor de 2 cm de las muestras que contenían caucho, como se corroboró mediante difracción de rayos X (DRX) y análisis termogravimétrico (TG). La transferencia de calor debida a la exposición al fuego modificó considerablemente la composición química de los revestimientos que contenían caucho, ya que, en la cara no expuesta al fuego, la cantidad de yeso ( $\text{CaSO}_4 \cdot 2\text{H}_2\text{O}$ ) equivalente a la pérdida de masa obtenida por TG debida al agua liberada por estos revestimientos, fue entre 5.4 y 7.2 veces inferior a la de los revestimientos de yeso convencionales. Los resultados sugieren que ciertos residuos pueden reducir la eficacia de los revestimientos de yeso en la protección de elementos constructivos y estructurales contra el fuego.

**PALABRAS CLAVE:** Yeso; Residuos de caucho de neumático; Fuego; Temperatura; Protección pasiva.

**Copyright:** ©2022 CSIC. This is an open-access article distributed under the terms of the Creative Commons Attribution 4.0 International (CC BY 4.0) License.

## 1. INTRODUCTION

Gypsum ( $\text{CaSO}_4 \cdot 2\text{H}_2\text{O}$ ) is a non-combustible material and has been widely used to provide structural and building elements with passive protection. The material has low thermal conductivity and contains crystallisation water that partially consumes the heat energy of fire by transformation into,  $\text{CaSO}_4 \cdot \frac{1}{2}\text{H}_2\text{O}$  also referred to as bassanite and, finally, its lowest hydrated form known as anhydrite,  $\text{CaSO}_4$ . Even after this dehydration, gypsum continues to act as a passive protection coating, preserving its fireproof features without emitting harmful gases or smoke.

In Spain, a considerable amount of End-of-Life Tires (ELT) are generated each year. A possible way to re-use tire wastes is to obtain granulated rubber particles that can be incorporated to a wide range of elements, as for instance bituminous materials for roads, football pitches, sports fields, or thermal and acoustic insulation panels among other uses. Similarly, gypsum-based products can be improved by incorporation of lightweight additions aimed at improving the workability of the final product as well as providing added thermal and acoustic insulation properties. However, the coating behavior to fire may be worsened along with important mechanical hardness features.

Among these additions are phase change materials (1), expanded clay, perlite, vermiculite and expanded polystyrene (2, 3). These materials can be incorporated into binding mixtures like mortars, renders and plasters. To counteract the deterioration of mechanical properties, some studies have used lightweight additions (EPS) and reinforcement materials, such as glass fibres (2) or polypropylene fibres, reducing density and increasing the flexural strength (4). The raising interest in reusing wastes from industrial sectors (e.g. construction and industry sector) has led to novel ideas for the incorporation of lightweight materials in rendering and plastering products. For example, recycled newspaper, printing paper and pine wood particles may improve the flexural strength of some materials (5). Another example is the incorporation of expanded polystyrene wastes in gypsum panels and boards (6-8), mixtures of expanded and extruded polystyrene wastes (9) or polyamide dust wastes into gypsum matrices (10). Likewise, the inclusion of laminated plasterboards residues (11) and the creation of composite materials made of rubber waste from pipe foam insulation (12) have been recently investigated.

Recycled crumb rubber was used as lightweight aggregate by N. Eldin *et al.* in 1993 in concrete (13). The material produces substantial reduction in the compressive strength, flexural strength and modulus of elasticity, but the tenacity of the material can be improved. In addition, numerous authors have studied the compatibility and adhesion of rubber grains to cementitious matrices (14-21), thermal behavior properties (22-26) and acoustic absorption features (26-28). However, little is known on the incorporation of recycled rubber

particles into gypsum materials like plasters. Mayor, P. *et al.* (29) studied the use as addition of recycled crumb rubber in plaster slabs. They used a single particle size in quantities of 20%, 30%, 40% and 50% by volume of the final product. As the amount of rubber increased, the mechanical strength and Young's modulus decreased, while thermal and acoustic characteristics of the slabs were improved. Serna, A. *et al.* (30) added small proportions of recycled crumb rubber to gypsum (between 1% and 5%) and used three different grain sizes (0-1 mm, 1-2 mm, 2-4 mm). They found that the flexural and compressive strength were decreased by 16% and 19.3%, respectively. Finally, Herrero del Cura, S. (31) analysed the influence of the dose and granulometry of recycled crumb rubber on thermal, acoustic and mechanical properties of gypsum-rubber plasters. In this case, the plaster became less homogenous and workable by increasing the rubber dose and the size of the grains. Also, the porosity increased and the material density was reduced (up to 47%), especially for the finest granulometries. Similarly, Shore C hardness, flexural and compressive strength were reduced when the dose of rubber was increased in the plasters. The reduced adhesion between the rubber grains and the gypsum matrix and the fact that rubber may interfere in the formation of crystalline structures commonly formed in gypsum materials may explain these results. In addition to better elastic behavior or deformability, the use of rubber in gypsum plasters leads to higher water absorption (capillary and immersion), and open porosity. Herrero del Cura, S. (31) also concluded that the inclusion of recycled crumb rubber improves acoustic insulation properties of plasters, although airborne noise reduction depends largely on the size of the rubber particles. The material may also improve the thermal insulation capacity of gypsum boards, obtaining the best results for the finest grain size (32, 33).

Gypsum plasters provide excellent passive protection of nearby materials, but little is known on the fire performance of gypsum plasters made with tire rubber wastes.

The aim of this work is to investigate the effect of tire rubber wastes in the fire behavior of gypsum plasters, with a major focus on textural and chemical modifications. For this purpose, SEM examination as well as XRD and TG measurements are used to assess the extent to which plasters containing rubber wastes are affected by fire.

## 2. EXPERIMENTAL PROCEDURE

### 2.1. Materials

#### 2.1.1. Binder

The gypsum binder ( $\text{CaSO}_4 \cdot \frac{1}{2}\text{H}_2\text{O}$ ) was supplied by a local manufacturer; the material is classified as

B1 according to the EN 13279-1 standard, which establishes the technical requirements that construction plasters must meet (34).

### 2.1.2. Additions

Worn-out tire wastes from mechanical crushing of used tires having a range size 0-0.5 mm were used as addition. The aggregates were supplied by a local producer and the physical-chemical features of the waste are summarized in Table 1.

TABLE 1. Physical-chemical characteristics of tire rubber waste.

Aspect	Granular material	
Particle geometry	Irregular	
Composition	Rubber 55 ± 5% Carbon black 32 ± 3% Acetone extract 7 ± 3% Ashes 4 ± 2 %	
Apparent density (g/cm <sup>3</sup> )	0.45 ± 0.05	
Color	Black	
Granulometry	<u>Sieve</u>	<u>% Retained</u>
	0.7 mm	< 1.5
	0.5 mm	5-25
	0.3 mm	35-55
	<0.3 mm	25-50

The gypsum plasters made with waste were coded as C1 and C2 and prepared with 14.50% and 46.60% by weight respectively of tire rubber (Table 2). The used percentages were chosen to achieve powdered densities around 0.800 g/cm<sup>3</sup> and 0.600 g/cm<sup>3</sup> to simulate low or very low density plasters. The samples were compared with control plasters (M0 samples), in which powdered density was 0.942 g/cm<sup>3</sup>.

TABLE 2. Composition and code of the studied plaster samples; tire rubber doses are given as mass percentage (w/w).

Powder product	w/s ratio	Code
100% binder (control)	1.0	M0
85.50% binder + 14.50% rubber waste	1.0	C1
53.40% binder + 46.60% rubber waste	1.0	C2

## 2.2. Methods

### 2.2.1. Preparation of specimens

The mixing and curing process was carried out according to the standard EN 13279-2 (35). The samples were mixed with regular water using constant water solid ratio (w/s) of 1.0. The ratio was adjusted to achieve suitable workability of plasters (especially when rubber aggregates were used). All

specimens were prepared with the same ratio for comparative purposes. As to the specimens' format, two types of samples were prepared; type 1, consisted of the usual prismatic specimens (40 x 40 x 160 mm) for testing mechanical properties and type 2, specimens necessary to conduct fire tests, with dimensions of 200 x 200 x 20 mm.

The specimens were cured for 90 days under laboratory conditions (23±3 °C and 55±10% HR). After this period, the samples were kept in an oven at 40 °C to achieve constant mass before conducting mechanical and characterization tests.

### 2.2.2. Density tests

The powder material was gently poured into a container having a known volume and previously weighed with an accuracy of 0.01 g. The density was obtained by dividing the net weight of the powdered material by the volume of the container. The same procedure was used for determining the density of the paste.

Similarly, the apparent density of the hardened gypsum was obtained from the type 1 specimens at 90 days of curing. In this case, the specimens were measured along each side with a caliper (±0.01 mm). The mass of the samples was obtained with weight-scale (±0.01g) and divided by the apparent volume, which was calculated from the average size.

### 2.2.3. Physical properties: Shore C hardness, flexural and compressive strength

Shore C hardness was measured taking into account the EN 13729-2 recommendations (35). To this aim, a Baxlo Shore C hardness device equipped with a reference material (60 Shore C units) was used. Three determinations were made on the lateral sides of the specimens to prevent possible errors associated to segregation and water flotation from the bottom to the top side of the specimens.

The flexural strength (Fs) was conducted by following the EN 13729-2 standard (35) in which the testing machine provides the load necessary to split the prismatic specimen into two sub-samples. The flexural strength Fs was obtained by the following formula;  $F_s = 0.00234 \times L$ , where L is the average breaking load for three repetitions (n=3).

The samples resulting from flexural tests were used for evaluating the compressive strength (Cs) according to the EN 13729-2 (35). As usual in compressive tests, the specimens were placed on 40 x 40 mm plates and the Cs was obtained from the expression:  $C_s = L_c / 1600$ , where Lc is the load to achieve failure and acting on a surface of 1600 mm<sup>2</sup> (n=6).

For both flexural and compressive strength tests, a Microtest EM2 electromechanical testing machine was used (±0.01 kN).

#### 2.2.4. Fire tests

The specimens were exposed to fire using a blow torch fed by propane gas, anchored to a mobile support with a graduated path, which was gradually moved from position 0 to position 5; the device remained in each position for 2, 3, 4, 5, 6 and 10 minutes, respectively (36). Through this procedure it was possible to vary the maximum temperature reached in the exposed face (EF) from room temperature to  $830 \pm 50$  °C. This maximum temperature was affected by convective processes of the flame and the nature of the additions tested.

At the same time, images of the non-exposed face (NEF) of the specimen were obtained using a thermographic camera (FLIR T400) in order to analyze both the temperature and heat distribution created by fire. For this, the specimens were placed on a stainless steel support and the fire protocol described above was applied, performing 30 minutes tests through which thermal images were recorded every minute with the thermographic camera attached to a tripod in a fixed position (Figure 1).

In addition, the temperature of the fire was measured on the exposed face (EF) by means of a chromel-alumel K type thermocouple located in the action center of the flame. In this case, thermographic measurements could not be used because the heat from the flame saturates the camera detector. An Omron ZR-RX 25 Data Logger was used to record the temperature measurements made by the thermocouple. Three tests per composition were carried out.

#### 2.2.5. Scanning electron microscopy analysis (SEM)

SEM images were captured from both unfired samples and those exposed to fire. For the latter samples, the two sides of the specimens i.e. the exposed face (EF) and non-exposed face (NEF) were also examined by SEM. The analyses were carried out with a Hitachi S-3500N scanning electron microscope working at a voltage of 15 kV and 2000 magnification in Backscattered Electrons mode (BSE).

#### 2.2.6. X-ray fluorescence analysis (XRF)

Gypsum powder samples were analysed by XRF. This test is used to obtain the percentage concentration of the elements that make up a material. A wavelength dispersive X-ray fluorescence spectrometer Bruker S4 Pioneer with an X-ray generation range of 20-60 kV and 5-150 mA was used.

#### 2.2.7. X-ray diffraction analysis (XRD)

Gypsum powder samples, unfired samples and samples taken from the exposed (EF) and non-exposed face (NEF) of the specimens subjected to fire were analysed by XRD. Since gypsum is sensitive to temperature, the aim of the study was to find out gypsum-related minerals that were stable at certain temperatures or fire conditions. To do this, the samples were gently ground in a mortar and the mineral phases were identified using the Cu K-alpha line using a Bruker D8 Advance powder diffractometer for powder analysis. A scan angle range (2-theta) of  $10^\circ$  to  $70^\circ$  with a resolution of  $0.05^\circ$  was used.

#### 2.2.8. Thermogravimetry analysis (TG)

Equally, gypsum powdered samples, samples of the unfired specimens and those obtained from the EF and NEF of the specimens subjected to fire were studied by thermogravimetric analysis TG, which measures the sample mass variation as a function of temperature or time. For this, a Mettler-Toledo TGA / DSC HT thermogravimetric analyzer was used and the temperature was progressively increased from room temperature to 1600 °C with an accuracy of  $\pm 0.5$  °C and a heating rate of 20 °C / min. The measurements were made using O<sub>2</sub> at a flow rate of 50 ml / min in the oven atmosphere. Taking advantage of the high sensitivity of TG analysis, the sampling was carefully made by eroding a few mg from the most superficial layer of the samples using a spatula.

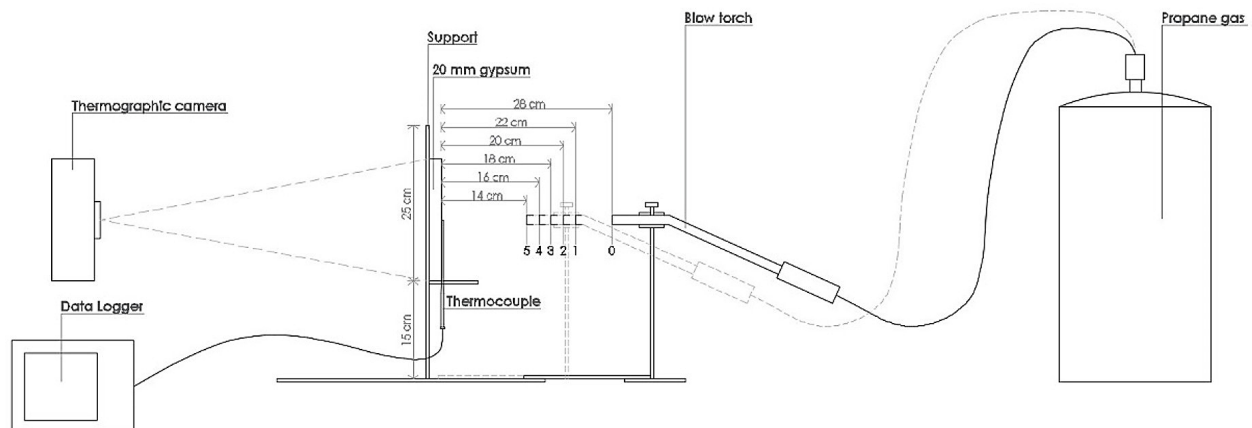


FIGURE 1. Diagram of the direct fire test components.

### 3. RESULTS AND DISCUSSION

#### 3.1. Binder and tire rubber waste characterization: XRD, XRF and TG

Preliminary XRD study carried out on powdered gypsum samples confirmed the existence of bassanite ( $\text{CaSO}_4 \cdot \frac{1}{2}\text{H}_2\text{O}$ ) as the main mineral of the binder with a much lower presence of anhydrite or anhydrous calcium sulfate ( $\text{CaSO}_4$ ), calcite ( $\text{CaCO}_3$ ) and dolomite ( $\text{CaMg}(\text{CO}_3)_2$ ) as can be seen in Figure 2. The small peaks of gypsum may be explained by natural hydration of the binder due to atmospheric factors (moisture).

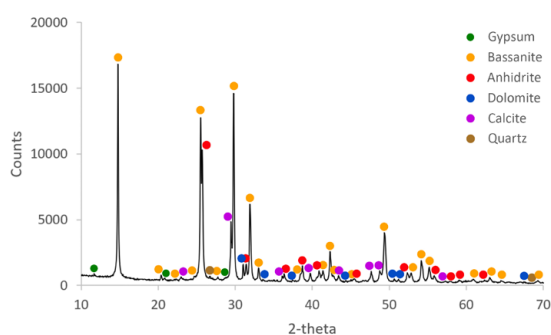


FIGURE 2. XRD of Binder B1.

Moreover, for binder B1, TG tests showed a first mass loss of 4.88% due to transformation of calcium sulfate hemihydrate ( $\text{CaSO}_4 \cdot \frac{1}{2}\text{H}_2\text{O}$ ) into anhydrite ( $\text{CaSO}_4$ ) at around 130 °C. Then, at around 670 °C a second mass loss (2.49%) is explained by decarbonation of calcite ( $\text{CaCO}_3$ ) due to  $\text{CO}_2$  evaporation ( $\text{CaO} + \text{CO}_2$ ) (Figure 3).

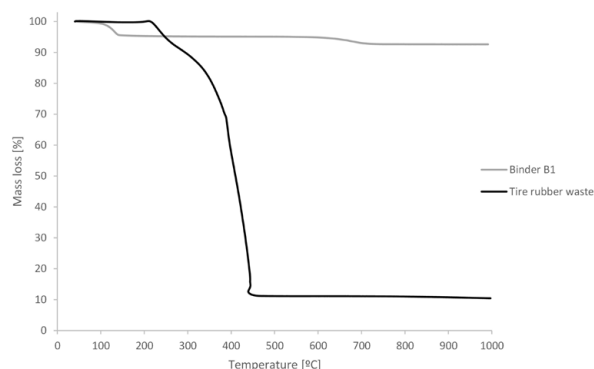


FIGURE 3. TG of binder B1 and tire rubber waste.

Finally, the binder was also studied by XRF analysis, from which the concentration of elements expressed as oxides was obtained and shown Table 3. As expected, the two major oxides were those associated with major elements of the binder i.e. Ca and

TABLE 3. XRF of binder B1.

Oxide	Concentration (%) Binder B1
$\text{H}_2\text{O}^*$	4.8772
$\text{CO}_2^*$	2.4943
MgO	0.80
$\text{Al}_2\text{O}_3$	0.38
$\text{SiO}_2$	1.19
$\text{SO}_3$	49.10
$\text{K}_2\text{O}$	0.16
CaO	40.47
$\text{TiO}_2$	0.02
$\text{Fe}_2\text{O}_3$	0.19
SrO	0.23
Other	0.90

\*:  $\text{H}_2\text{O}$  and  $\text{CO}_2$  were determined by TG.

S. The amount of  $\text{SiO}_2$  is explained by common minerals like quartz often present in sedimentary rocks and also reported by XRD. In addition, the small concentration of MgO suggests that minerals associated to Mg (e.g. dolomite) have very little influence on the total amount of carbonates, which are mainly present as calcite. The  $\text{H}_2\text{O}$  and  $\text{CO}_2$  concentration was not determined by XRF, but obtained from TG since this technique has greater sensitivity and reliability for detecting low atomic number elements due to their low X-ray absorption.

XRD analysis carried out on tire rubber waste confirmed the existence of zincite ( $\text{ZnO}$ ) as the main mineral phase with a rather minor presence of quartz ( $\text{SiO}_2$ ) and calcite ( $\text{CaCO}_3$ ) (Figure 4). The diffractogram also indicates, on the left part, the amorphous nature of some components like carbon black added to tires. Besides, Zn-based compounds are most likely related to de-molding agents added to tires in their manufacturing and processing (21).

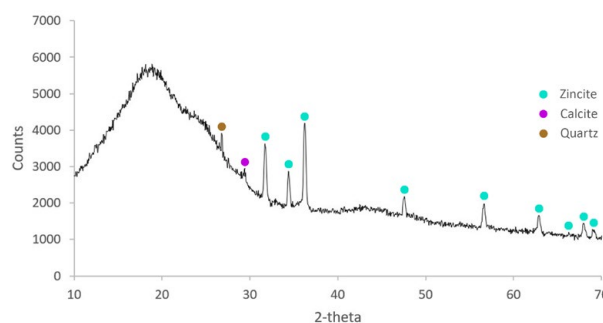


FIGURE 4. XRD of tire rubber waste.

Rubber waste particles were also studied by TG analysis. In this case, rubber oxidation along with carbon black combustion ( $C+O_2 = CO_2$ ) were clearly observed in the thermogram. Although both processes are partially overlapped in the TG curve, the first mass loss found at around 250 °C (9.66%) is probably due to organic matter decomposition from rubber constituents followed by a major step of 80.30% at around 400 °C, in which rubber oxidation is completed ( $CO_2$  and  $H_2O$ ) together with carbon combustion ( $CO_2$ ). Lastly, S from vulcanization may also contribute to oxidation and mass loss due to  $SO_3$  release (Figure 3).

SEM examination carried out on the surface of tire rubber grains revealed the heterogeneous aspect of the waste (Figure 5a). At low magnification (100x) the particle size of most grains matches well the range specified by the manufacturer (0.5 mm). At higher magnifications (1000x) an irregular relief and dissimilar chemical phases with punctual brightness from elements of higher atomic number than carbon can be seen (Figure 5b).

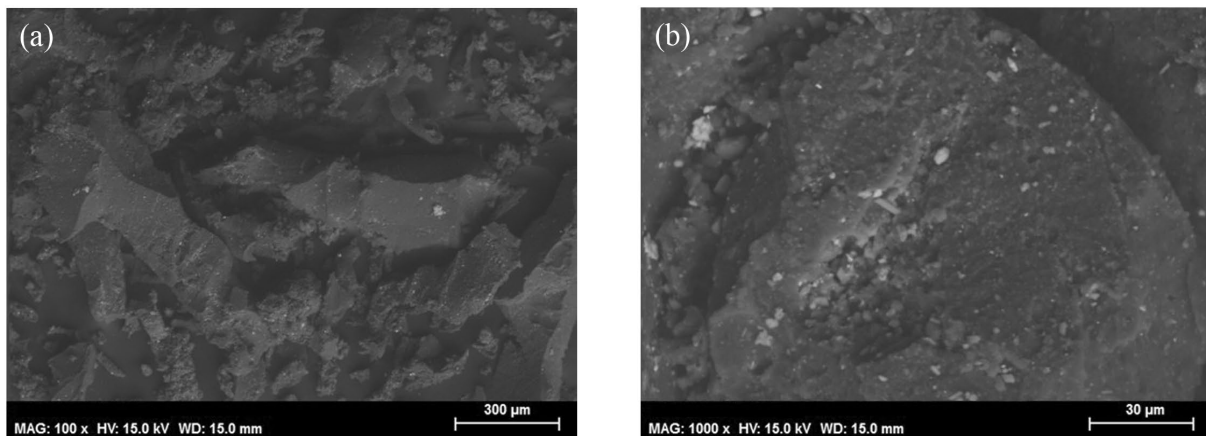


FIGURE 5. SEM images of tire rubber waste.

TABLE 4. Density, Shore C hardness and mechanical strength of plasters.

Mix code.	Powder density, g/cm <sup>3</sup>	Fresh density, g/cm <sup>3</sup>	Hardened density, g/cm <sup>3</sup>
M0	0.942	1.415	0.843
C1	0.800	1.276	0.759
C2	0.600	1.002	0.669
Mix code.	Shore C, units (n = 18)	Flexural strength, MPa (n = 3)	Compressive strength, MPa (n = 6)
M0	57.7 ± 0.7	1.83 ± 0.16	4.80 ± 0.17
C1	34.9 ± 0.5	0.83 ± 0.08	2.20 ± 0.22
C2	11.9 ± 1.0	0.28 ± 0.04	0.66 ± 0.05

### 3.2. Physical properties: density, hardness and mechanical strength

One of the advantages of adding tire rubber waste to plasters is to obtain a lighter materials due to the low density of the waste in comparison with conventional aggregates used in plasters. Table 4 shows indeed a substantial reduction of density in powdered, fresh and hardened state and the mechanical features of plasters made with tire rubber waste.

The values obtained for the physical properties are in accordance with the trends shown in the existing literature (29-31). Basically, the plasters became lighter and mechanically weaker.

### 3.3. Fire tests

Recycled crumb rubber is a material of organic nature with moderate thermal conductivity, but combustible and hence, it contributes to fire spread and generates gases too. For this reason, the use of tire rubber wastes in plasters may cause substantial dam-

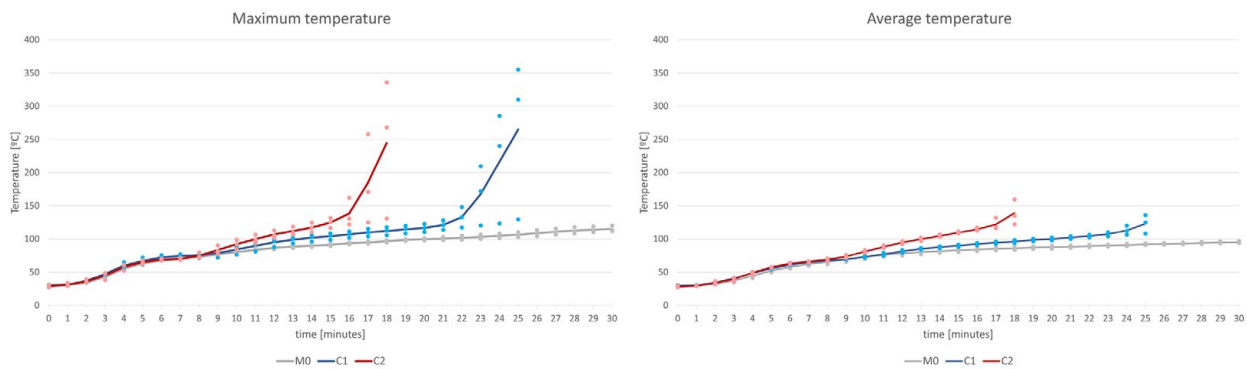


FIGURE 6. Temperatures recorded on the NEF.

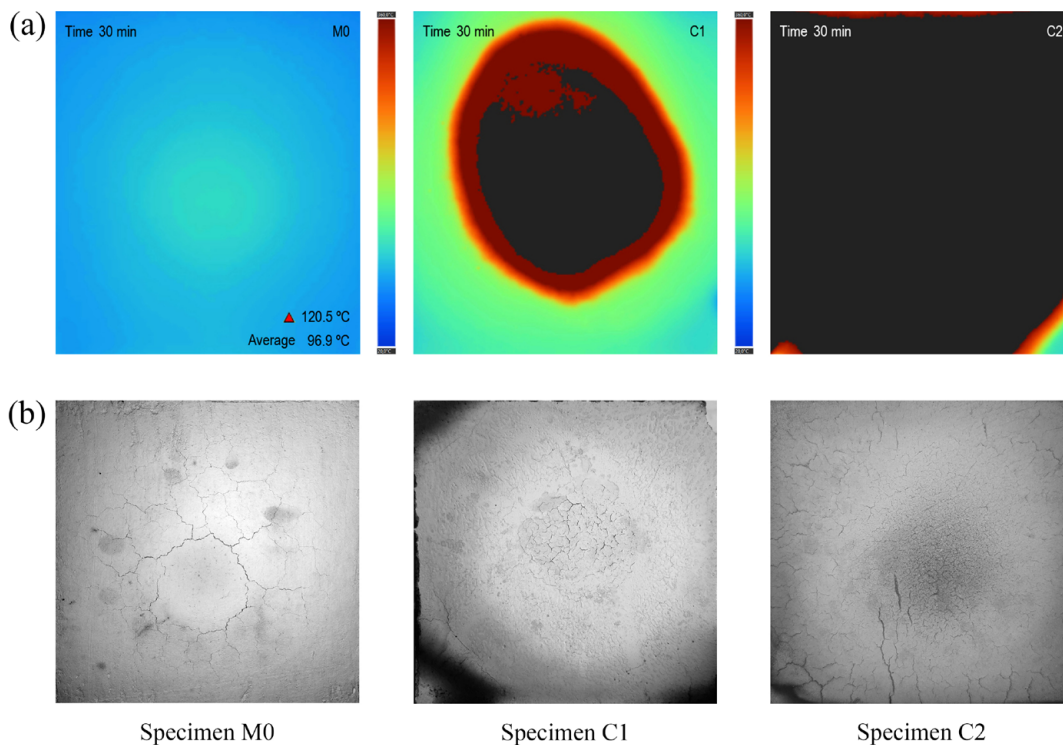


FIGURE 7. (a) Temperatures recorded on the NEF; (b) Cracking of specimens on the EF.

age of nearby materials like concrete due to chemical and microstructural alterations induced by fire. This section aims to evaluate to what extent plasters made with tire rubber wastes are suitable materials when exposed to intense fire.

Figure 6 shows the maximum and average temperature variation recorded in the non-exposed face (NEF) of specimens using thermographic camera. As can be seen in the graph, at the beginning of the test, the maximum temperature of the specimens containing rubber (C1 and C2) is slightly higher than that recorded for the reference sample M0. After 8 minutes, the maximum temperature recorded in the NEF of C1 and C2 specimens increases significant-

ly in comparison to M0 samples. Indeed, for both doses there is a much faster increase of maximum temperature in the final part of the test. For C1 samples, the maximum temperature rises drastically at around 22 minutes for two of the specimens and the third one presents some delay (25 minutes). In almost 3 minutes, the temperature rise is of the order of 200 °C. For C2 samples, this occurs earlier at approximately 15-17 minutes depending on the tested specimen. In both doses, the temperature increases rapidly and exceeds the maximum temperature detectable by the thermographic camera (360 °C) in a few minutes. This sudden increase is explained by rubber combustion. In addition, for C2 dose, ig-

tion in some of specimens occurs, producing an added heat transfer due to fire. Therefore, although rubber wastes may reduce the thermal conductivity of building materials (31), its contribution to fire is actually an important drawback. The same trend was found by recording the average temperature on the NEF with C2 sample being again the most affected.

Figure 7a shows thermographic images for the NEF of M0, C1 and C2 samples after 30 minutes of fire exposure. Each image provides in the upper right corner the composition of the specimen. These images show a temperature map of the fire NEF of several gypsum specimens (with or without tire rubber waste) of 2 cm thickness that could be assimilated to equivalent commonly used gypsum coatings of similar thickness. The images provide clarifying information on what takes place 2 cm behind the plaster, where other building materials like brick or concrete are usually located in real situations. At 30 min, the black color indicates zones of C1 and C2 samples where the maximum temperature detectable by the camera IR sensor (360 °C) was reached.

Clearly, the combustion and exothermic oxidation of crumb rubber plays a major role in transferring the heat to the NEF.

Moreover, the EF of the specimens was examined after completing the tests. All samples M0, C1 and C2 showed crack patterns due to microstructural and mineral alterations caused by fire. The pattern differs considerably as M0 showed less cracks, but wider cracks spacing than C1 and C2 (Figure 7b). The pattern is consistent with a more rigid behavior of M0 in comparison to plasters made with elastomeric wastes as C1 and C2 samples (31).

### 3.4. Scanning electron microscopy (SEM) analysis

Figure 8 shows SEM images of M0, C1 and C2 plasters before and after being subjected to fire. In general, the addition of tire rubber grains had visible effect on microstructural features of gypsum. In samples non-exposed to fire (M0), the matrix is composed of acicular crystals having different crys-

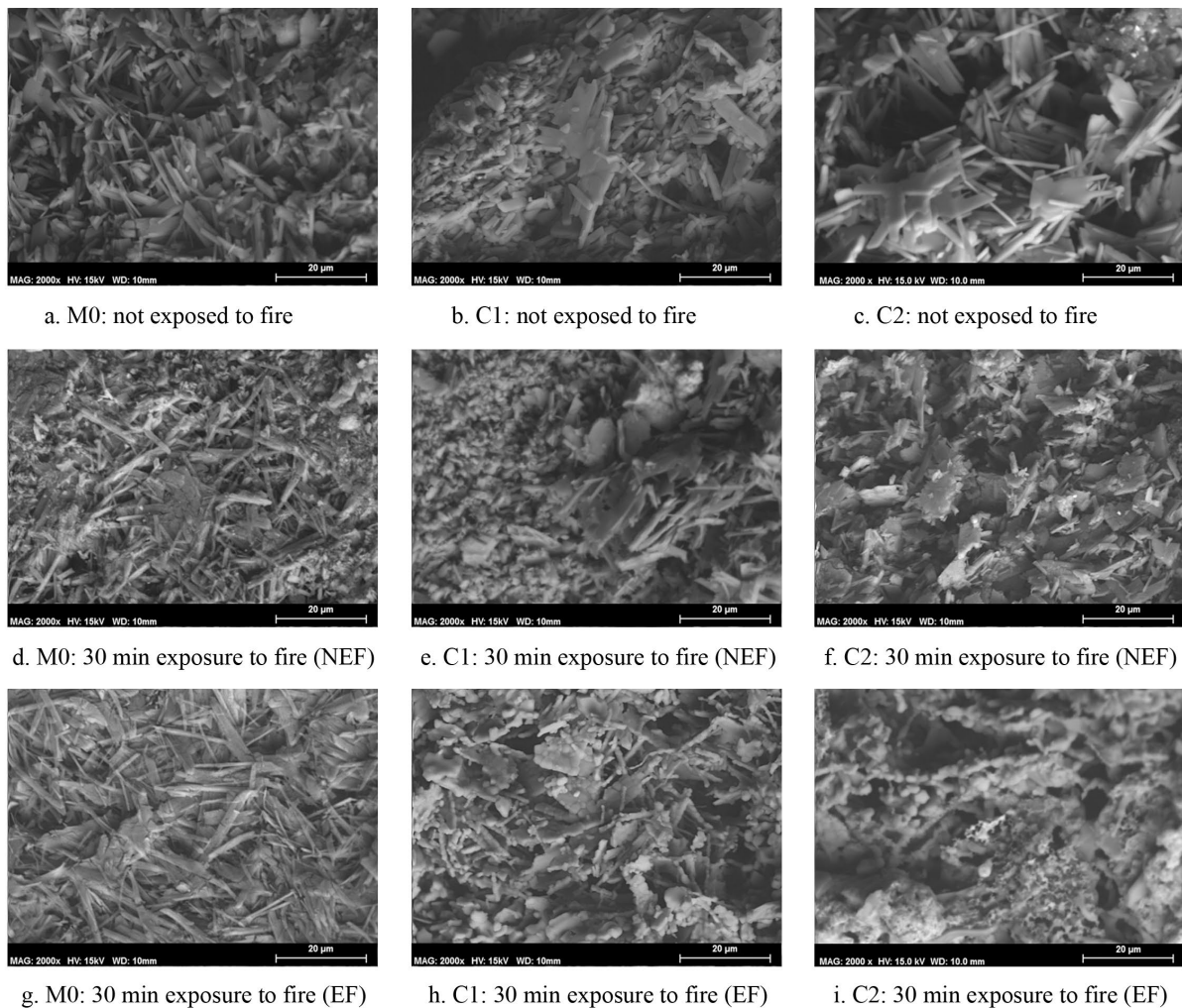


FIGURE 8. Images SEM.

talline habits and morphologies as usual for gypsum (Figure 8a). In C1 and C2 samples, the rubber particles produce minor changes decreasing the binding capacity of gypsum (Figure 8b and 8c). The poor adhesion between rubber and gypsum crystals may reduce the plaster's mechanical strength, as earlier discussed in Table 4 and previous studies (29-31).

SEM examination also confirmed that samples exposed to fire were visibly affected, and particularly those plasters containing tire rubber wastes. Despite the destructive nature of fire tests, the elongated shape of gypsum is easily recognized in M0 samples, especially in the NEF, as they resisted fire better than C1 or C2 (Figure 8 d-f). This is consistent with the thermographic data because the average temperature of the NEF did not exceed 100 °C in M0 samples.

By contrast, in samples containing rubber (C1 and C2), the crystals became shorter and more heterogeneous with a major fraction of crystals resembling bassanite or anhydrite shapes (habits) due to the higher temperatures reached in the NEF (>360 °C). As regards the EF, the temperatures recorded with the thermocouple being around 830±50 °C and the

samples were clearly affected, although the microstructural changes were again more perceptible in C1 and C2 samples (Figure 8 g-i).

### 3.5. X-ray diffraction analysis (XRD)

The XRD pattern of M0 unfired samples (Figure 9a) showed the material contains gypsum as main mineral ( $\text{CaSO}_4 \cdot 2\text{H}_2\text{O}$ ) and minor proportions of bassanite ( $\text{CaSO}_4 \cdot \frac{1}{2}\text{H}_2\text{O}$ ), anhydrite ( $\text{CaSO}_4$ ), calcite ( $\text{CaCO}_3$ ), dolomite ( $\text{CaMg}(\text{CO}_3)_2$ ) and quartz ( $\text{SiO}_2$ ). No major differences were found between M0, C1 and C2 unfired samples (Figure 9c and 9e), except that the magnitude of certain peaks associated to gypsum in C2 was slightly reduced due to the diluting effect of the addition. Besides, the large amount of rubber added to this sample increased the background signal (baseline) because of the amorphous nature of the waste.

The XRD analyses were repeated after exposing the samples to fire for comparison purposes. The study was carried out on both sides of the specimens

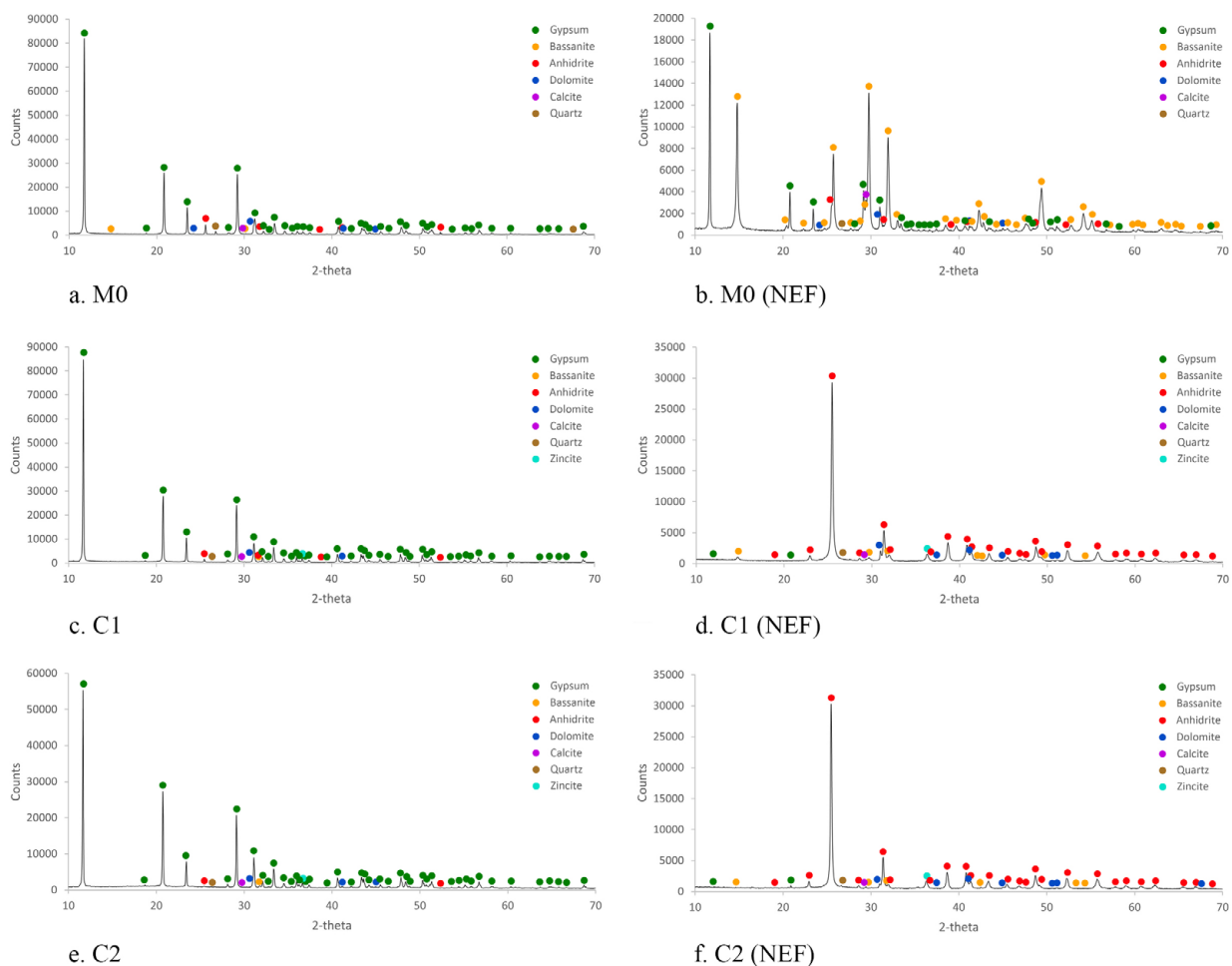


FIGURE 9. XRD of specimens not tested and tested on fire during 30 minutes (NEF).

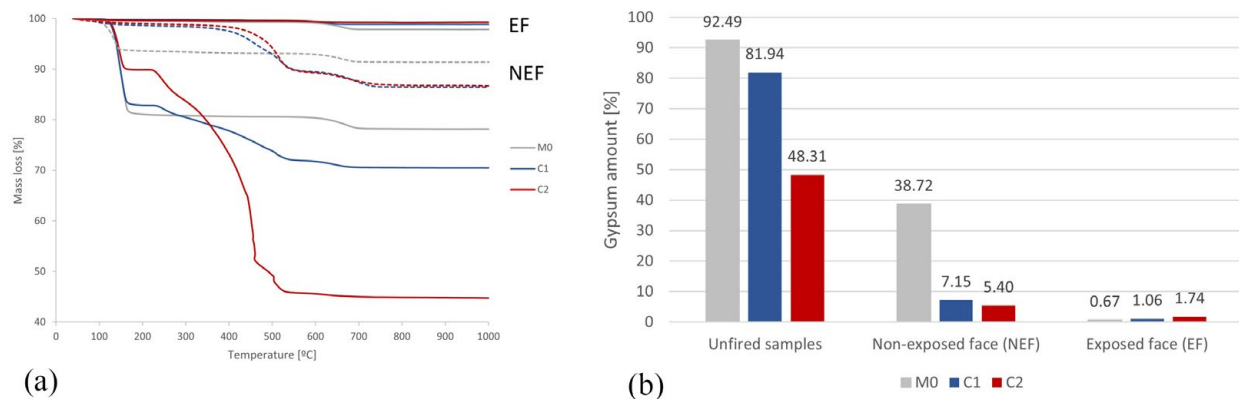


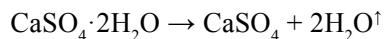
FIGURE 10. (a) TG; (b) Percentage of gypsum in unfired samples and samples exposed to fire during 30 minutes.

to check the effect of temperature on the mineral phases. In the NEF of M0 sample, the semi-hydrated form (bassanite) increased clearly at the expense of gypsum (Figure 9b). In addition, the presence of anhydrite remains the same, which is in agreement with temperature measurements performed in the non-exposed face. No differences were observed in thermally stable minerals like quartz or those much more stable than gypsum, such as calcite and dolomite. However, in C1 and C2 samples, the vast majority of gypsum was transformed into anhydrite and only small peaks of bassanite were observed (Figure 9d and 9f). This corroborates the poor fire performance of tire rubber additions when added to gypsum plasters.

The minerals found in the exposed face to fire (EF) of M0, C1 and C2 indicate that for this fire exposure time practically all the gypsum in all the samples has been converted into anhydrite.

### 3.6. Thermogravimetry analysis (TG)

The concentration of certain components can be evaluated by TG and particularly, the decrease in gypsum concentration due to anhydrite conversion is an accurate indicator to evaluate fire severity. In the thermogram (Figure 10a), the first mass loss is due to water released from gypsum according to the following reaction:



Although the reaction takes place in two steps, they are overlapped in a single one and completed within 100-200 °C. In addition, this temperature range is clearly lower than the initial decomposition of tire rubber wastes. Thus, the first step of the thermogram was used to evaluate the amount of  $\text{CaSO}_4 \cdot 2\text{H}_2\text{O}$  in all samples using stoichiometric calculations summarized below:

Molecular mass of gypsum ( $\text{CaSO}_4 \cdot 2\text{H}_2\text{O}$ ):  
172.17 g/mol

Molecular mass of water released in the reaction:  
 $18.0148 \cdot 2 = 36.0296$  g/mol

Percentage of water in  $\text{CaSO}_4 \cdot 2\text{H}_2\text{O}$ : 20.9268 (%)

Percentage of mass loss in the first step (water released): X (%)

Percentage of gypsum ( $\text{CaSO}_4 \cdot 2\text{H}_2\text{O}$ ) in the sample:  $X \cdot 100 / 20.9268$  (%)

Figure 10b shows the percentage of gypsum in unfired and fired samples. In unfired samples, the amount of gypsum decreases because of the mentioned dilution effect of tire rubber wastes (C1 and C2). It is worth noting that the binder also contains minor proportions of dolomite (4.15%) and calcite (0.98%) measured by semi-quantitative XRD analysis. Therefore, the reported percentage of gypsum in C1 and C2 samples (81.94% and 48.31%) is consistent with the initial concentration of binder in the samples (85.50% and 53.4%). Equally, the amount of gypsum (92.49%) resulting from hydration of unfired M0 samples indicates the purity of the binder.

However, the percentage of gypsum was visibly reduced in samples subjected to fire either in the exposed or non-exposed face of plasters. In the non-exposed face, M0 presented better behavior to fire than samples made with rubber wastes (C1 or C2). In fact, the percentage of gypsum in M0 samples (38.72%) was between 5.4-7.2 times greater than that of C1 and C2. Anyway, it is clear that the heat propagation through the entire 2 cm thickness of M0, C1 and C2 specimens provoked an important destruction of binder (gypsum). As expected, the face exposed to fire was, by far, much more affected since the gypsum percentage was nearly residual, and below 1.8% in all samples.

## 4. CONCLUSIONS

This paper evaluates the physical performance and fire behavior of gypsum plasters made with tire rubber wastes (C1 and C2) and conventional plasters

(M0). As a result of the investigation, the following conclusions can be drawn:

The addition of tire rubber wastes to gypsum plasters (C1 and C2) presents practical advantages in terms of density reduction producing pastes that are both easily applied. However, the waste produces important physical modifications and the plasters are mechanically weaker. For instance, the flexural strength of plasters decreased by 55-85%, the compressive strength decreased by 54-86% and the same is true for Shore C hardness tests (40-80% approximately).

It is worth stressing that despite the low combustibility of gypsum, the incorporation of tire rubber worsens considerably the plasters behavior to fire. For instance, thermographic measurements using IR camera shows that the temperature of the non-exposed face of plasters containing tire rubber (C1 and C2) rises much more rapidly than that of control plasters (M0). This is an important concern as gypsum plasters play a major role in the passive protection against fire of building and structural materials (e.g. concrete). It is worth noting that the developed methodology uses instrumental techniques for determining the effect of fire in the composition of plasters. Nevertheless, the fire resistance classification of plasters or their contribution to fire as defined by international standards is out of the scope of the present study.

As expected, the exposed face undergoes visible microstructural changes and major chemical modifications in all samples (M0, C1 and C2). In addition to morphological alterations observed by SEM, it was found that gypsum is practically consumed due to the intense action of fire as confirmed by XRD and TG.

In the non-exposed face, conventional plasters (M0) having usual thicknesses (2 cm) provide good behavior to fire. Indeed, despite the extreme conditions to which the samples were subjected (about  $830 \pm 50$  °C in the exposed face), the underneath layers (2 cm below) remain relatively well preserved after 30 min of fire. The integrity of the non-exposed face is proven by temperature measurements, and also XRD and TG data confirming the existence of hydrated minerals like gypsum and bassanite.

By contrast, the concentration of gypsum drops considerably in tire rubber plasters exposed to fire (C1 and C2). For example, XRD tests performed at the non-exposed face confirm that gypsum ( $\text{CaSO}_4 \cdot 2\text{H}_2\text{O}$ ) is almost completely transformed into anhydrite ( $\text{CaSO}_4$ ). Likewise, quantitative determinations carried out by TG analysis in the non-exposed face are consistent with the above findings as the gypsum percentage is clearly reduced in samples containing tire rubber wastes.

#### AUTHOR CONTRIBUTIONS:

Conceptualization: F.J. Castellón, M. Ayala, M. Lanzón. Data curation: F.J. Castellón, M. Ayala, M. Lanzón. Formal analysis: F.J. Castellón, M. Ayala, M. Lanzón. Investigation: F.J. Castellón,

M. Ayala, M. Lanzón. Methodology: F.J. Castellón, M. Ayala, M. Lanzón. Resources: F.J. Castellón, M. Ayala, M. Lanzón. Software: F.J. Castellón, M. Ayala, M. Lanzón. Supervision: M. Lanzón. Validation: F.J. Castellón, M. Ayala, M. Lanzón. Visualization: F.J. Castellón, M. Ayala, M. Lanzón. Writing, original draft: F.J. Castellón, M. Ayala, M. Lanzón. Writing, review & editing: F.J. Castellón, M. Ayala, M. Lanzón.

#### REFERENCES

1. Oliver, A. (2009) Tesis Doctoral. Integración de materiales de cambio de fase en placas de yeso reforzadas con fibras de polipropileno. Aplicación a sistemas de refrigeración y calefacción pasivos para almacenamiento de calor latente en edificios. Universidad Politécnica de Madrid.
2. Del Río Merino, M. (1999) Tesis Doctoral. Elaboración y aplicaciones constructivas de paneles prefabricados de escayola aligerada y reforzada con fibra de vidrio E y otros aditivos. UPM.
3. Del Río Merino, M.; Domínguez, J.D.; Hernández Olivares, F. (1998) Escayola aligerada con sólidos celulares. *Inf. Constr.* 50 [468], 43-60. <https://doi.org/10.3989/IC.1998.V50.I458.878>.
4. García Santos, A. (2009) Escayola reforzada con fibras de polipropileno y aligerada con perlas de poliestireno expandido. *Mater. Construcc.* 59 [293], 105. <https://doi.org/10.3989/mc.2009.41107>.
5. Haselein, C.R. (2002) Fabricação de chapas de partículas aglomeradas usando gesso como material cimentante. *Cienc. Florest.* 12 [1], 81-87. <https://doi.org/10.5902/198050981703>.
6. González Madariaga, F.J. (2005) Tesis Doctoral. Caracterización de mezclas de residuos de poliestireno expandido (EPS) conglomerados con yeso o escayola, su uso en la construcción. UPC.
7. González Madariaga, F.J. (2008) Mezclas de residuos de poliestireno expandido (EPS) conglomerados con yeso o escayola para su uso en la construcción. *Inf. Constr.* 60, [509], 35-43.
8. De Oliveira, K.A.; Oliveira, C.A.B.; Molina, J.C. (2021) Lightweight recycled gypsum with residues of expanded polystyrene and cellulose fiber to improve thermal properties of gypsum. *Mater. Construcc.* 71 [341], e242. <https://doi.org/10.3989/mc.2021.07520>.
9. Del Río Merino, M.; Villoria-Sáez, P.; Longobardi, I.; Astorqui, J.S.C.; Porras-Amores, C. (2019) Redesigning lightweight gypsum with mixes of polystyrene waste from construction and demolition waste. *J. Clean. Produc.* 220, 144-151. <https://doi.org/10.1016/j.jclepro.2019.02.132>.
10. Gutierrez, S.; Gadea, J.; Rodríguez, A.; Blanco-Varela, M. T.; Calderón, V. (2012) Compatibility between gypsum and polyamide powder waste to produce lightweight plaster with enhanced thermal properties. *Constr. Build. Mater.* 34, 179-185. <https://doi.org/10.1016/j.conbuildmat.2012.02.061>.
11. Rodríguez-Orejón, A.; Del Río Merino, M.; Fernández-Martínez, F. (2014) Characterization mixtures of thick gypsum with addition of treated waste from laminated plasterboards. *Mater. Construcc.* 64, [314]. <https://doi.org/10.3989/mc.2014.03413>.
12. Jiménez Rivero, A.; De Guzmán Báez, A.; García Navarro, J. (2014) New composite gypsum plaster-ground waste rubber coming from pipe foam insulation. *Constr. Build. Mater.* 55, 146-152. <https://doi.org/10.1016/j.conbuildmat.2014.01.027>.
13. Eldin, N.; Senouci, A. (1993) Rubber-tire particles as concrete aggregate. *J. Mater. Civ. Eng.* 5 [4], 478-496. [https://doi.org/10.1061/\(ASCE\)0899-1561\(1993\)5:4\(478\)](https://doi.org/10.1061/(ASCE)0899-1561(1993)5:4(478)).
14. Khabit, Z.K.; Bayomy, F.M. (1999) Rubberized portland cement concrete. *J. Mater. Civ. Eng.* 11 [3], 206-213. [https://doi.org/10.1061/\(ASCE\)0899-1561\(1999\)11:3\(206\)](https://doi.org/10.1061/(ASCE)0899-1561(1999)11:3(206)).
15. Toutanji, H.A. (1996) The use of rubber tire particles in concrete to replace mineral aggregates. *Cem. Concr. Compos.* 18 [2], 135-139. [https://doi.org/10.1016/0958-9465\(95\)00010-0](https://doi.org/10.1016/0958-9465(95)00010-0).
16. Fedroff, D.; Ahmad, S.; Savas, D.Z. (1996) Mechanical properties of concrete with ground waste tire rubber. *Transp.*

- Res. Rec.* 1532, 66-72. <https://doi.org/10.1177/0361198196153200110>.
17. Segre, N.; Joeke, I. (2000) Use of tire rubber particles as addition to cement paste. *Cem. Concr. Res.* 30 [9], 1421-1425. [https://doi.org/10.1016/S0008-8846\(00\)00373-2](https://doi.org/10.1016/S0008-8846(00)00373-2).
  18. Li, G.; Stubblefield, M.A.; Garrick, G.; Eggers, J.; Abadie, C.; Huang, B. (2004) Development of waste tire modified concrete. *Cem. Concr. Res.* 34 [12], 2283-2289. <https://doi.org/10.1016/j.cemconres.2004.04.013>.
  19. Albano, C.; Camacho, N.; Reyes, J.; Feliu, J.L.; Hernández, M. (2005) Influence of scrap rubber addition to portland I concrete composites: Destructive and non-destructive testing. *Compos. Struct.* 71 [3-4], 439-446. <https://doi.org/10.1016/j.compstruct.2005.09.037>.
  20. Hernández Olivares, F.; Barluenga, G.; Bollati, M.; Witoszek, B. (2002) Static and dynamic behaviour of recycled tyre rubber-filled concrete. *Cem. Concr. Res.* 32 [10], 1587-1596. [https://doi.org/10.1016/S0008-8846\(02\)00833-5](https://doi.org/10.1016/S0008-8846(02)00833-5).
  21. Lanzón, M.; Cnudde, V.; De Kock, T.; Dewanckele, J. (2015) Microstructural examination and potential application of rendering mortars made of tire rubber and expanded polystyrene wastes. *Constr. Build. Mater.* 94, 817-825. <https://doi.org/10.1016/j.conbuildmat.2015.07.086>.
  22. Hernández Olivares, F.; Barluenga, G. (2002) Fire performance of recycled rubber-filled high-strength concrete. *Cem. Concr. Res.* 34 [1], 109-117. [https://doi.org/10.1016/S0008-8846\(03\)00253-9](https://doi.org/10.1016/S0008-8846(03)00253-9).
  23. Turatsinze, A.; Bonnet, S.; Granju, J.L. (2005) Mechanical characterisation of cement-based mortar incorporating rubber aggregates from recycled worn tyres. *Built. Environ.* 40 [2], 221-226. <https://doi.org/10.1016/j.buildenv.2004.05.012>.
  24. Benazzouk, A.; Douzane, O.; Mezreb, K.; Laidoudi, B.; Quénuédec, M. (2007) Thermal conductivity of cement composites containing rubber waste particles: Experimental study and modelling. *Constr. Build. Mater.* 22 [4], 573-579. <https://doi.org/10.1016/j.conbuildmat.2006.11.011>.
  25. Turgut, P.; Yesilata, B. (2009) Investigation of thermo-mechanical behaviors of scrap added mortar plate and bricks. *J. Faculty Engineer. Architec. Gazi Univ.* 24 [4], 651-658.
  26. Sukontasukkul, P. (2009) Use of crumb rubber to improve thermal and sound properties of pre-cast concrete panel. *Constr. Build. Mater.* 23 [2], 1084-1092. <https://doi.org/10.1016/j.conbuildmat.2008.05.021>.
  27. Khaloo, A.R.; Dehestani, M.; Rahmatabadi, P. (2008) Mechanical properties of concrete containing a high volume of tire-rubber particles. *Waste Manage.* 28 [12], 2472-2482. <https://doi.org/10.1016/j.wasman.2008.01.015>.
  28. Flores Medina, D.; Flores Medina, N.; Hernández Olivares, F. (2014) Static mechanical properties of waste rests of recycled rubber and high quality recycled rubber from crumbed tyres used as aggregate in dry consistency concretes. *Mater. Struct.* 47, 1185-1193. <https://doi.org/10.1617/s11527-013-0121-6>.
  29. Mayor Lobo, P.; Bustamante Montoro, R.; Rangel, C.; Hernández Olivares, F. (2008) Propiedades térmicas, acústicas y mecánicas de placas de morteros de yeso-caucho. *II Jornadas de Investigación en Construcción*, Madrid, Instituto de Ciencias de la Construcción Eduardo Torroja.
  30. Serna, A.; Del Río Merino, M.; Palomo, G.; González, M. (2012) Improvement of gypsum plaster strain capacity by the addition of rubber particles from recycled tyres. *Constr. Build. Mater.* 35, 633-641. <https://doi.org/10.1016/j.conbuildmat.2012.04.093>.
  31. Herrero del Cura, S. (2016) Tesis Doctoral. Influencia de la dosificación y granulometría del caucho de neumáticos fuera de uso (NFU) y de las dimensiones físicas en las propiedades térmicas, acústicas y mecánicas de placas de mortero yeso-caucho. UPM.
  32. Abu-Lebdeh, T.; Fini, E.; Fadiel, A. (2014) Thermal conductivity of rubberized gypsum board. *J. Eng. Appl. Sci.* 7 [1], 12-22. <https://doi.org/10.3844/ajeassp.2014.12.22>.
  33. Pinto, N.; Fioriti, C.; Akasaki, J.; Acunha, T.; Okimoto, F. (2020) Performance of plaster composites incorporating rubber tire particles. *Rev. Ing. Construcc.* 35 [2], 215-231. <http://doi.org/10.4067/S0718-50732020000200216>.
  34. UNE-EN 13279-1 (2009) Yesos de construcción y conglomerantes a base de yeso para la construcción. Parte 1: Definiciones y especificaciones, AENOR.
  35. UNE-EN 13279-2 (2014) Yesos de construcción y conglomerantes a base de yeso para la construcción. Parte 2: Métodos de ensayo, AENOR.
  36. Castellón, F.J.; Ayala, M.; Flores, J.A.; Lanzón, M. (2021) Influence of citric acid on the fire behavior of gypsum coatings of construction and structural elements. *Mater. Construcc.* 71 [342], e248. <https://doi.org/10.3989/mc.2021.13120>.